New satellite observations and the cloud parameterization problem

Graeme L Stephens

Department of Atmospheric Sciences
Colorado State University, Ft Collins, CO

1. Introduction

Representing cloudiness in global forecast models is complex and correctly treating the radiative and hydrological processes in the cloudy atmosphere in these models is particularly challenging. On the one hand, the atmospheric circulation is fundamental to these processes as synoptic scale motions in the atmosphere shape the planets cloudiness. These motions are well resolved in global models. However, the properties that determine the how much radiation is absorbed and reflected by clouds or how much water falls from clouds as precipitation are defined on a much smaller scale by processes that are typically not resolved by models. Therefore these cloud processes have to be approximated in ways that express them in terms of resolved large-scale model quantities. The approaches in dealing with clouds in this way and the problems associated with it are referred to as the 'cloud parameterization' problem.

Cloud parameterization typically follows two paths. Convective parameterization primarily focuses on representing the effects of convection in moistening and warming the large-scale atmospheric environment. Sub-grid scale convective parameterization generally produces the majority of the precipitation calculated by most global models, especially at low latitudes. Large-scale cloud parameterization properties are parameterized in terms of the thermodynamic and dynamical fields resolved by the model. One of the main functions of these parameterizations is to serve as input to the calculation of the model radiation budget although large-scale clouds also produce precipitation. The connections between convective clouds and radiative processes tend to be empirical.

2. New Global Observations of clouds and precipitation

The International Cloud Climatology Project (ISCCP) has provided important global observations of cloudiness from radiometric data collected from operational satellites since 1984. These data are now used in a number of ways in evaluation of global cloudiness. One example is in the cluster analysis introduced by Jakob and Tselioudis (2003). This analysis is a convenient way of grouping cloud information in categories and then relate the properties of clouds in these categories to other properties, like precipitation, and radiation. Perhaps more popular today is the use of the ISCCP simulator applied to model fields that can in turn be analyzed into the ISCCP histogram. The study of Webb et al (2002) is an example of how this simulator is used to contrast the effects of clouds on the TOA radiative fluxes as observed from ISCCP and ERBE and as represented in models. While these studies provide some means of evaluating models, cloud parameterizations per se can only be evaluated in a very indirect ways and not without ambiguity. The need for more direct measurement of cloud properties that offers a much deeper level of evaluation was one of the reasons CloudSat was developed.

2.1. CloudSat Objectives

The science objectives (Stephens et al., 2002) proposed for this mission revolved around the long recognized need to better represent cloud processes in global predictive models of weather and climate, specifically because: (i) clouds grossly affect the energy balance of the planet, and changes to cloud properties can entirely offset or greatly enhance effects of greenhouse gas induced warming; and (ii) the precipitation that falls from clouds is the fundamental source of freshwater that sustains life, and better prediction of clouds is essential for improving our ability to predict how precipitation patterns vary with, and might change with, changing weather and climate. Many of the key cloud properties relevant to these important issues are, to first order, governed by the vertical structure of clouds. For example, the degree to which clouds radiatively heat or cool the atmosphere depends on the height of the clouds and whether cloud layers are located above or below them. Whether or not clouds produce precipitation and the amount of precipitation produced and the latent heating created are directly related to the depths of clouds. The ability of clouds to warm the surface through emission of radiation depends on the height of cloud bases and so, too, is the potential water holding capability of clouds, which grossly affects the sunlight reflected by clouds to space. Thus the need to measure the vertical structure of clouds was paramount in the development of the mission.

The mission was launched April 28th, 2006 and since June, 2 2006 data has been collected operationally with almost no effective disruption.

2.2. Mission Characteristics

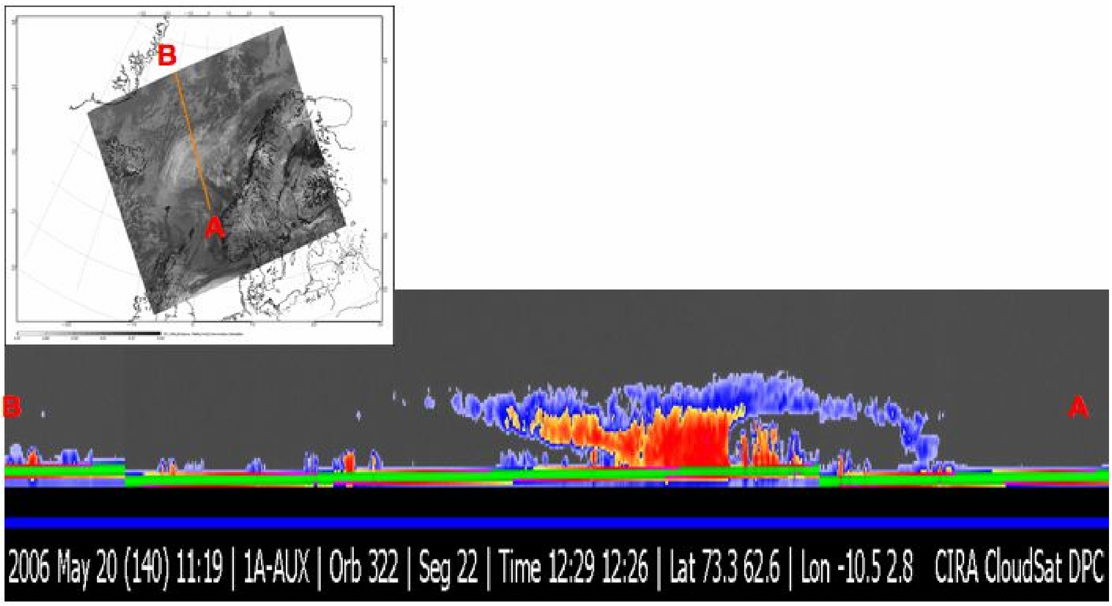

Figure 1 The first image of the CPR showing an approximate 1400km segment through a warm front observed over the Nth Atlantic on May 20th, 2006. The vertical scale runs from the surface (green line) to about 30km to top of image.

The **Cloud Profiling Radar (CPR)**: The science requirements, derived from the goals of the mission, led to the specification of a nadir-pointing radar system operating at 94 GHz – a wavelength of 3 mm with minimum sensitivity of -26 dBZ at end of life (EOL). However, the CPR, on-orbit, is performing significantly above expectation, achieving a minimum sensitivity between -30 and -31 dBZ , which is approximately 5 orders of magnitude more sensitive than that of the TRMM radar. The CPR can be expected to operate for several years before approaching the EOL sensitivity. The sensitivity and dynamic range mean that the CPR provides observations ranging from thin clouds to heavy, deep precipitating cloud systems. The first image obtained when early on-orbit tests were performed on May 20th is shown in Fig. 1

CloudSat Formation Flying And The A-Train: Although the intrinsic value of the CloudSat radar measurements alone is substantial, the value in combining data sets from other satellite sources was recognized from the outset. Matching the unique vertical radar information of CloudSat with other satellite data provides an opportunity to evaluate cloud products derived from more conventional, passive, radiance data. Given these obvious benefits, CloudSat was designed with a formation-flying element to enable matching of CloudSat observations closely in time with other more conventional satellite observations. CloudSat flies in the A-Train constellation, which includes the EOS Aqua and Aura at each end of the constellation, CALIPSO, and PARASOL. The original goal of the CloudSat formation flying architecture was to overlay the radar footprints on the lidar footprints of CALIPSO at least 50% of the time, as well as to ensure that the radar footprints fall in a fixed position with respect to the MODIS swath. Analysis indicates that this goal has been achieved with overlap occurrence of radar and lidar footprints >90% exceeding the goal. In this way CloudSat has demonstrated formation flying to be a practical observing strategy for future Earth observations.

3. Selected early results from CloudSat

3.1. Cloud vertical structure – global distributions

Figure 2 summarizes the overall hydrometeor coverage through the depth of the troposphere as well as the layer base and top coverage in 3 height ranges during June-August 2006. This figure illustrates the unique view that CloudSat provides of the vertical distribution of hydrometeor occurrence in the global atmosphere. For instance, it has not been possible with conventional observations to depict the distribution of layer base – a quantity that is fundamental to constraining the radiative balance of the surface radiation budget. Together with layer top and overall hydrometeor coverage, a unique rendering of the hydrometeor distribution in the atmosphere is produced.

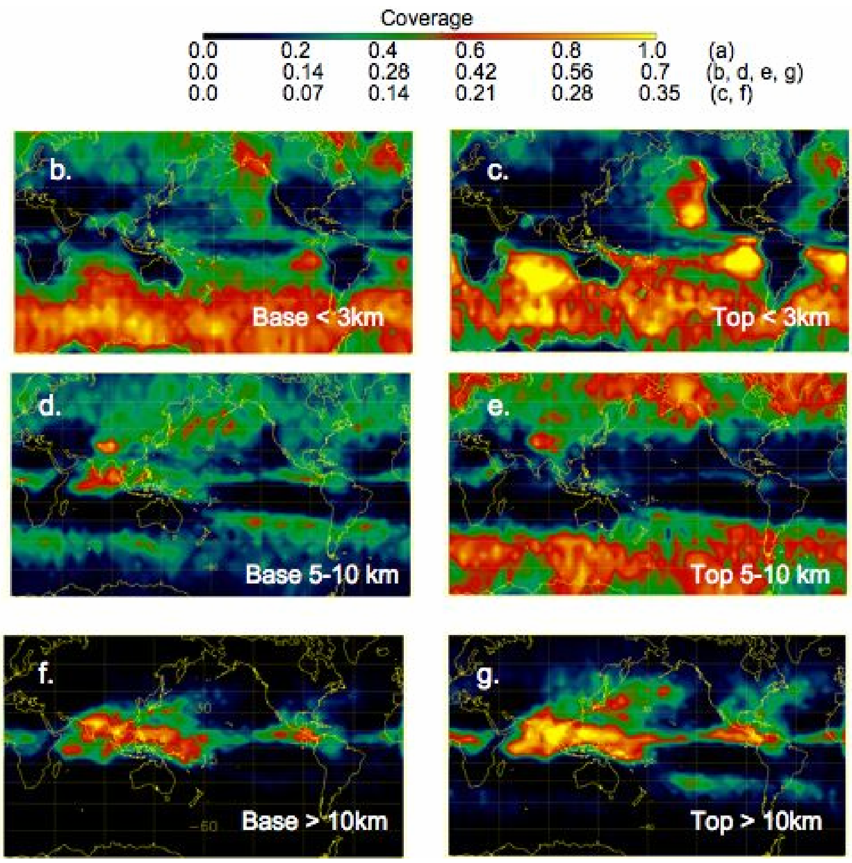

Figure 2 Hydrometeor coverage derived from CloudSat data collected during June, July, and August, 2006. 4º Latitude by 6º Longitude spatial averaging is used. a) Total hydrometeor coverage, b-g) Layer base and top coverage as specified in each figure. Note that the value assigned to the colors vary as specified for each figure (Mace et al., 2007).

3.2. Cloud vertical structure – tropical cloudiness

Haynes and Stephens (2007) review the vertical structure properties of tropical clouds. Averaged profiles of cloud maximum (left panels) and minimum (middle panels) top heights and the distribution of path integrated attenuation (PIA, right panels) are shown in Fig. 3. The latter related directly to preciptation. The profiles are normalized by the total incidence of total non-precipitating clouds (solid) and total precipitating clouds (dashed). These profiles reveal that the global tropics is characterized broadly by two layers of clouds, shallow clouds with maximum occurrence of cloud tops around 2 km and a second pronounced maximum near 12 km. Hints at the third mode near 7 km are also evident. The difference between precipitation and non-precipitating clouds (solid and dashed curves) is also remarkable. Precipitating shallow clouds are approximately 1 km deeper than the non-precipitating shallow clouds (middle panels) and deep precipitating clouds are approximately 2 km deeper than non-precipitating deep clouds. Also striking are the regional differences in the vertical distributions of cloud tops. The western Pacific appears to contain four modes, the shallow and deep modes already noted and two congestus modes with tops between 5-6 km and near 8km. The congestus mode is also evident in the Atlantic, less so in the eastern Pacific and is practically non-existant for clouds over the Indian Ocean.

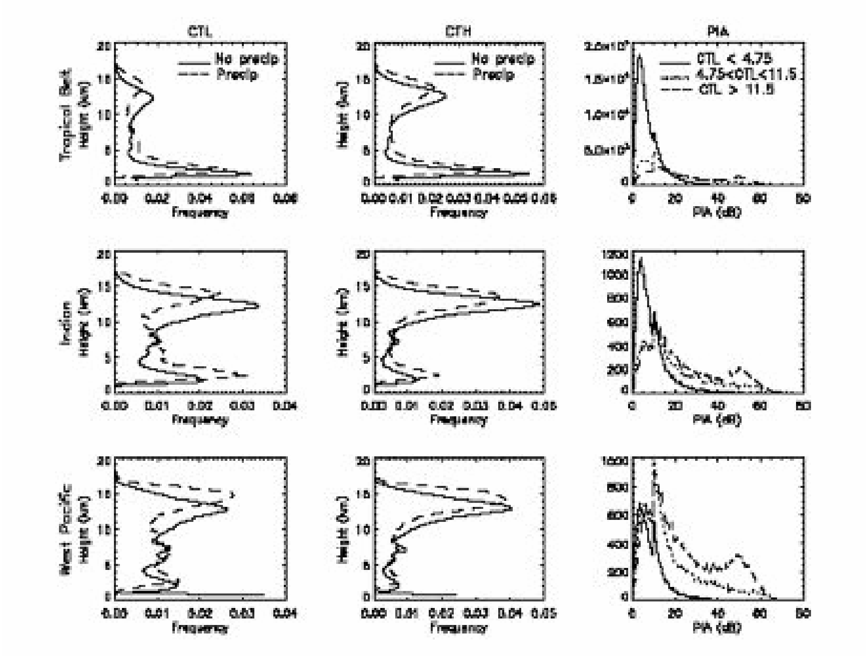

Figure 3Vertical profiles of the incidence of lowest layer cloud top height (CTL, left) and highest layer cloud top height (CTH, center) for the regions indicated. The solid line applies to all clouds and the dashed to precipitating clouds. Each profile is normalized by the total occurrence of the respective cloud type. The panels shown in the right column are the distributions of PIA for the three CTL height categories. The results are shown for the global tropics (upper) the western pacific region (middle) and the Indian Ocean (lower).

The distributions of PIA also hint at a number of remarkable features about the precipitation that falls from the clouds of these regions. As noted earlier, the frequency distribution of precipitation is bi-modal with the most frequent, shallow mode being characterized by low values of PIA with a peak value near 5 dB which is characteristic of light precipitation. The PIA distribution of the middle-level mode of cloudiness is bimodal with a maximum coinciding with the shallow maximum, a second maximum between 15-20 dB and a the long tail of even larger PIAs (and heavier precipitation). Deep precipitating clouds exhibit a more bimodal PIA distribution with a maximum between 15-20 dB similar to that observed for the congestus mode and a secondary maximum near 50 dB.

3.3. The Incidence Of Precipitation – an early measure of precipitation efficiency

The CloudSat radar is sensitive to the presence of precipitation, and the development of quantitative precipitation information from the radar observations is ongoing. Figure 4 illustrates one of the advantages jointly observations of clouds and precipitation in studying the planets hydrological cycle. This figure summarizes, in histogram form for JJA in selected regions over tropical oceans, the frequency of occurrence of clouds contrasted against the frequency of occurrence of clouds with detectible precipitation. The numbers refer to the fractions of all clouds that contain detectible precipitation being a crude indicator of the precipitation efficiency of cloud systems. This ratio varies between 0.13 and 0.18, with a minimum over the Indian Ocean and a maximum over the western Pacific region. Discovery of such variation is of profound importance to our understanding of the planet's hydrological cycle and ultimately important for predicting patterns of precipitation and precipitation variability.

More definitive studies of the variability of this sort of information are ongoing in an attempt to examine the environmental factors (like aerosol, sea surface temperature, etc) that possibly control this most elementary aspect of the cycling of water in our atmosphere.

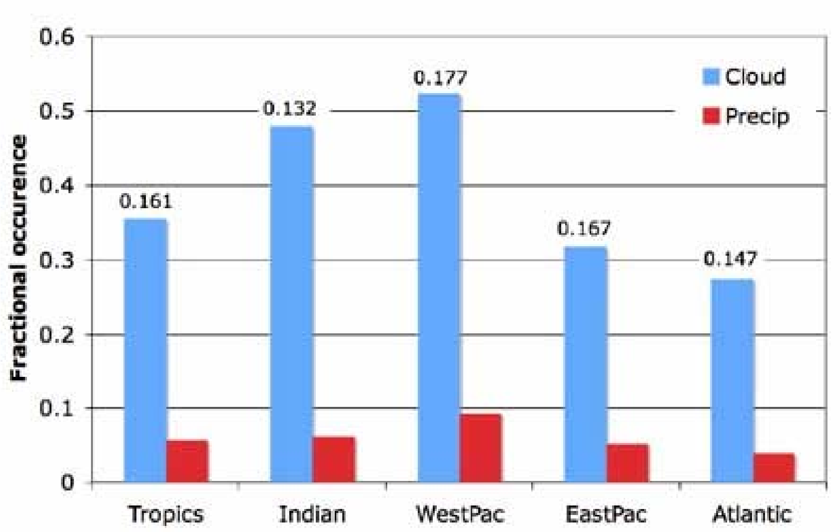

Figure 4 CloudSat offers a glimpse at the precipitation efficiency of clouds on the global scale, revealing tantalizing differences from region to region. The blue bars represent the frequency of occurrence of clouds observed by CloudSat during JJA and the red bars represent the percentage of those clouds that produce precipitation. The numbers above the blue bars refer to the ratio of the precipitating clouds to total clouds.

One of the longstanding, unanswered questions in atmospheric sciences is the question of what fundamentally determines the time scale between initial cloud formation and the onset of precipitation in warm clouds. Put simply, precipitation tends to develop more rapidly in the real world than is predicted from elementary theories about particle growth to warm rain. This is of fundamental significance to most aspects of weather and climate sciences as it determines how much water remains in clouds, their lifecycle, how aerosol influence clouds and the rate by which clouds cycle water through the atmosphere. Parameterization schemes developed for weather and climate models to represent the process by which cloud water is converted to rain are rudimentary, and untested on the scales of relevance to such models. The critical parameter of the schemes used in models is a timescale of the auto-conversion process. Classical particle growth theory suggests this is of order a few hours.

A completely novel approach to observe the warm rain process has been developed using combinations of Cloudsat and MODIS data. Figure 5 shows the rate of rain water production derived from matched CPR and MODIS observations as a function of cloud water. This relation identifies a range of time scales more rapid than theory suggests but consistent with observational experience. This is a significant result that should provide a new constraint on the tuning of parameterizations of warm rain in global models. The result also has implications on our understanding of the auto-conversion process and how other environmental factors (such as aerosol) might influence it.

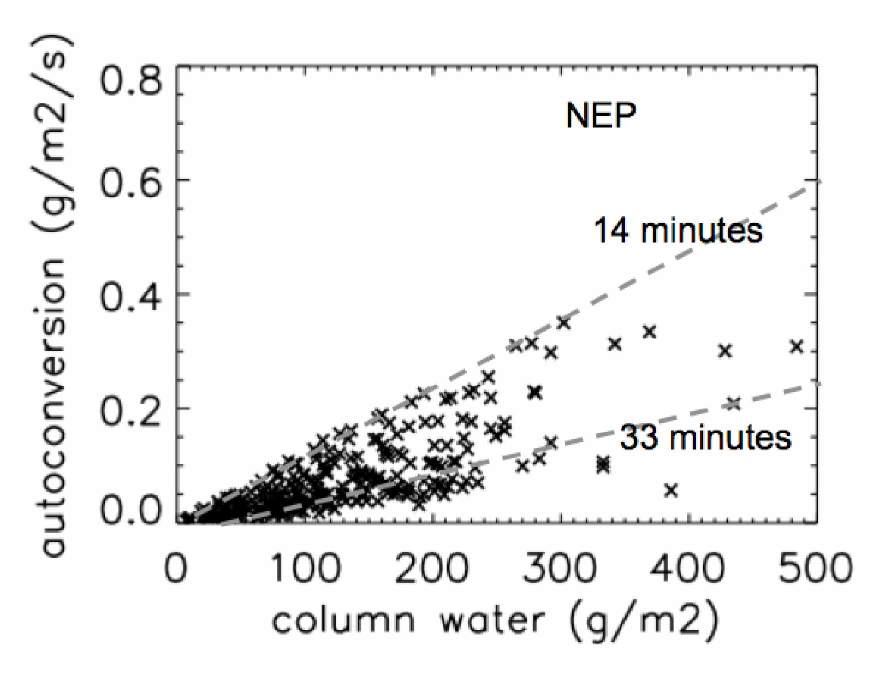

Figure 5: The relation between auto-conversion and cloud water for a large area of the North Eastern Pacific. The dashed lines imply a time scale for the turn-over of cloud water to rain water. This time scale is a critical untested parameter in most global model representations of the hydrological cycle.

4. Early comparison to models

An important goal of the CloudSat effort is to partner with major modeling groups and use the data to evaluate the model parameterizations of moist physics with the aim to improve this component of the model. The comparison of the new observations with models is just beginning.

4.1. Precipitation incidence

Figure 6 shows the frequency of precipitation grouped by three cloud-top height ranges where the height corresponds to that at which precipitation originates. When the same analysis of clouds and precipitation is performed on outputs from weather forecast models, remarkable differences emerge between model and observations, such as the lack of precipitation in weather forecast models for clouds with tops between 5 and 10 km in regions where deep convection occurs and too much precipitation associated with deep convection. The extent to which this precipitation mode is missing in other weather and climate models is also under study. The implication is that this may be an important mode of convective heating that is largely missing from models.

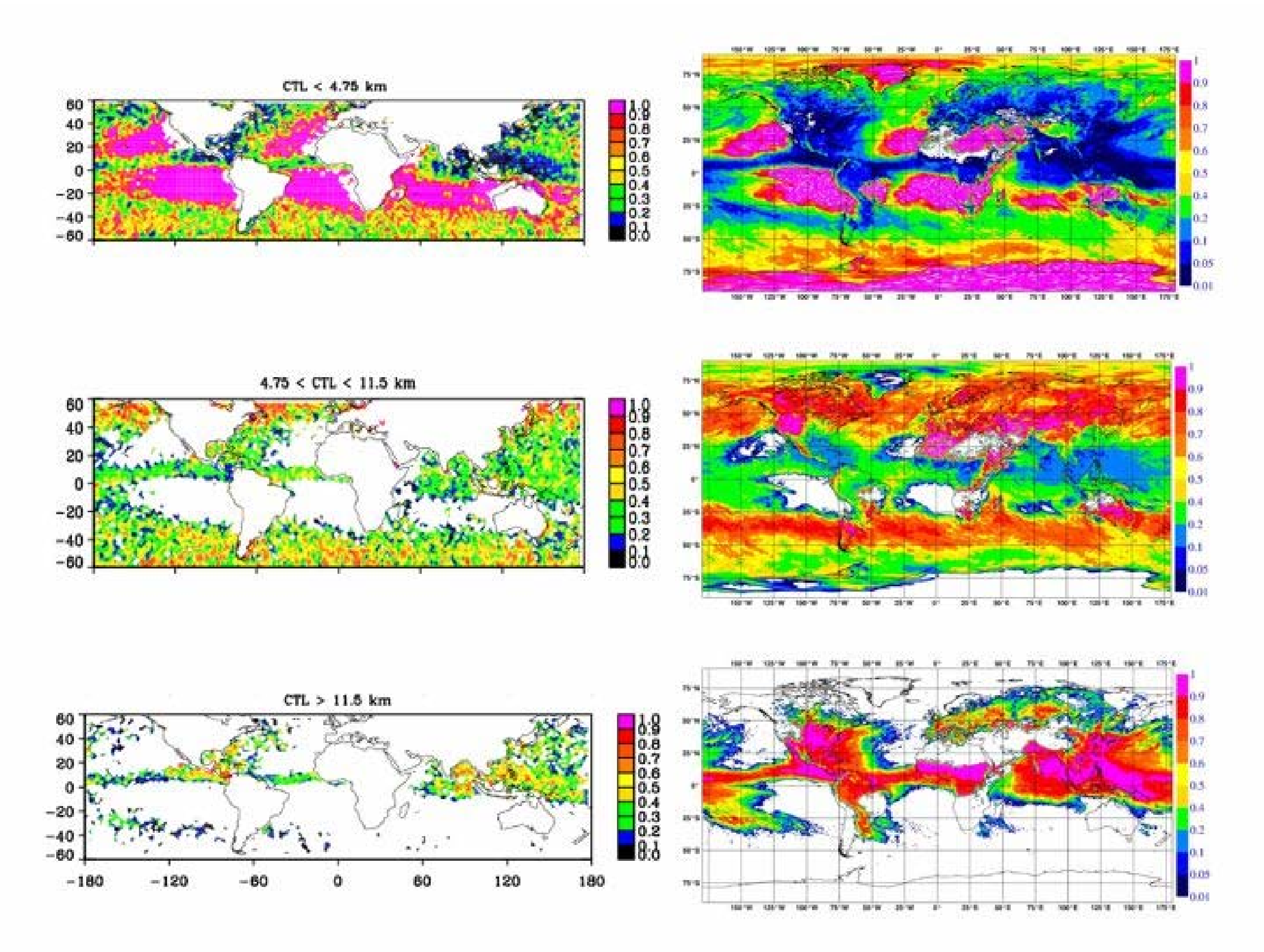

Figure 6 CloudSat observations are advancing the understanding and modeling of Earth's hydrological cycle. The three vertically stacked panels show the frequency of occurrence of precipitation binned by cloud-top height. This is a dramatic example of the unique ability of CloudSat to observe clouds and precipitation jointly. (b) The occurrence of precipitation from a weather forecast model. The differences are dramatic.

4.2. Constraining And Improving Ice And Water Contents Of The Atmosphere In Weather And Climate Models

The water contents of clouds are the quantities predicted by cloud-process and global-scale models, and when combined with the vertical structure, the water contents determine much of the important cloud properties, including precipitation and cloud optical properties. Water contents in models are highly parameterized and contain significant uncertainties which, for the most part, have not been quantified globally. The situation with prediction of ice-water contents of clouds is especially relevant. Prior to CloudSat and the A-Train, there were no real global measurements of ice to constrain models, and consequently the model-to-model variation in this quantity is astonishingly large (a factor of twenty between existing state-of-art climate models as used in the recent IPCC fourth assessment) despite the fact that the radiation balances of these models appear to be realistic in comparison to CERES measurements. There are many reasons why the lack of agreement between models is so disconcerting. The presence and amount of ice in the upper troposphere fundamentally affects the planet's greenhouse effect and profoundly influences atmospheric stability which also feeds back on convection and the strength of the hydrological cycle.

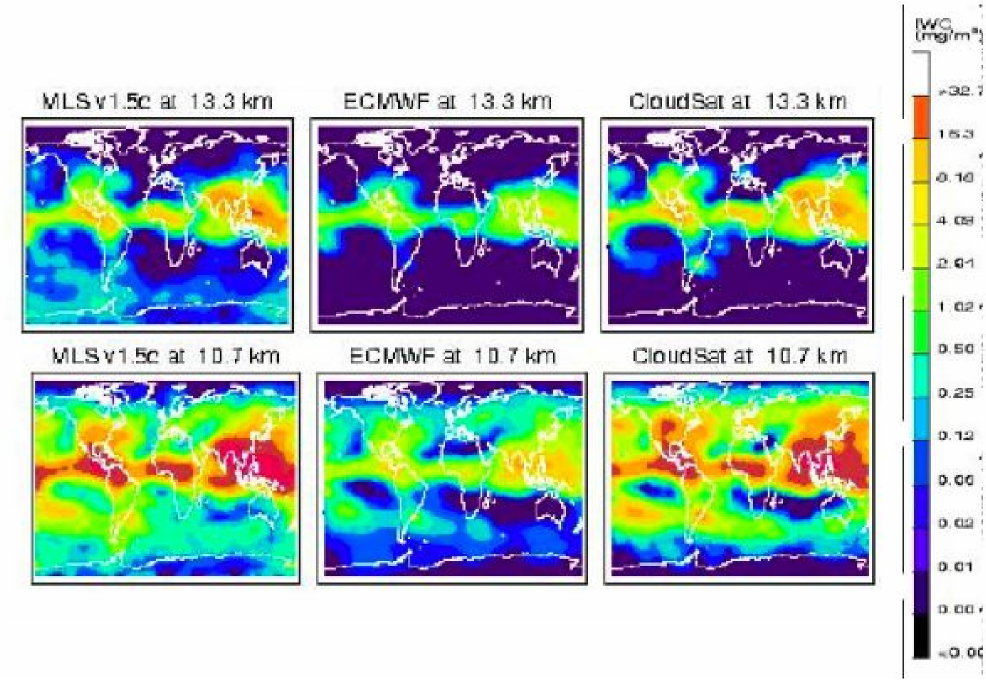

Figure 7 IWC maps from MLS and ECMWF with an early release version of the 2B-CWC CloudSat cloud-water-content product, at 10.7 and 13.3 km altitudes for the period 7 July-16 August 2006.) The overall cloud ice distribution in these maps is qualitatively similar, although the model values (ECMWF) indicate a profound bias that varies between factors of 2-5, implying shortfalls of model moist physics (Wu et al., 2007).

4.3. CloudSat radar simulator

To compare modeled clouds to the new observations being made by CloudSat, a radar simulator has been developed (Haynes et al., 2007). An example of application of the simulator to a GCM is shown in Fig. 4. Here the simulator is applied to the output of the UK Met Office global forecast model, which has a horizontal resolution of approximately 40 km at mid-latitudes. The sub-grid sampling approach described above has been applied and the grid-box mean radar reflectivity then obtained by averaging. The figure shows a transect through a mid-latitude depression in the North Atlantic on July 7th, 2006. The upper panel shows the analysis chart valid at 18 UTC, with the approximate CloudSat track in red, from point A near the Azores to point B off the south-east coast of Greenland. CloudSat passed over a mature mid-latitude system that was travelling eastwards in the North Atlantic, first crossing the warm front and then the core of the system, near the occluded front. The middle panel shows the radar reflectivity from CloudSat (dBZ), while the lower panel shows the simulated radar reflectivity. The contour lines in the lower panel are isothermals, the solid line denoting the freezing level. The vertical structure of the frontal system is very well represented by the model, which captures the deepening of high clouds as we approach the core of the system. This is dominated by large-scale precipitation which is also reasonably well represented by the model. However, the model produces too much high-level cloud that extends towards the south (left in the image), beyond the area where it is present in the observations and also produces low-level drizzling clouds in the warm sector beneath the high cloud, which are not observed by CloudSat. A detailed analysis of the application of the simulator to evaluation of cloud systems in the Met Office global forecast model is in progress.

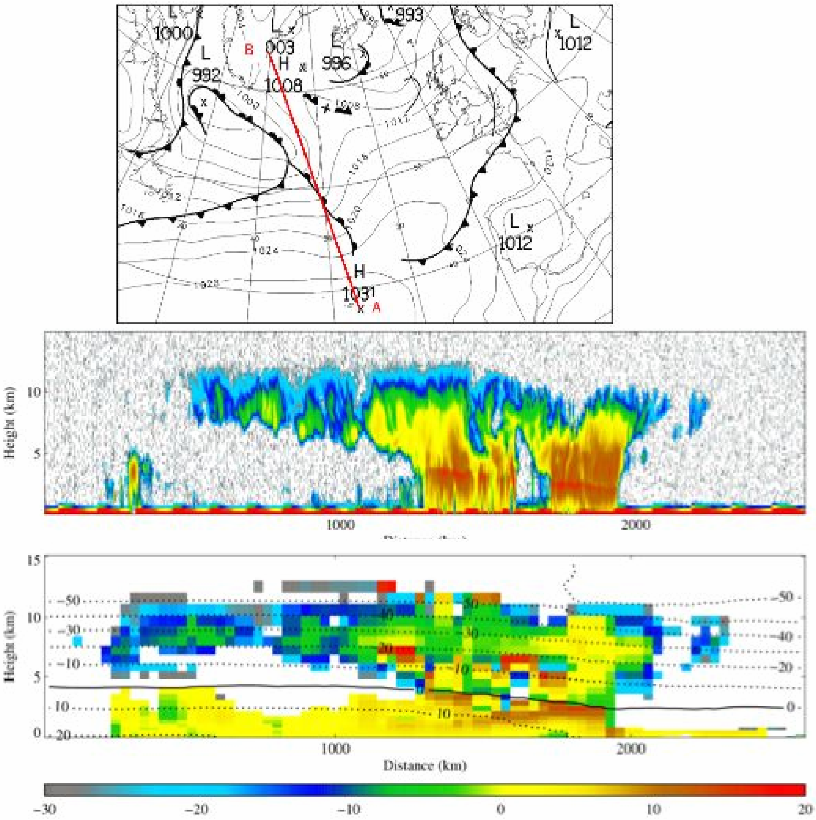

Figure 8 Example of simulated mid-latitude system in the UK Met Office global forecast model. The upper panel is the north Atlantic analysis chart at 18UTC on July 7th, 2006. The red line shows the CloudSat track, from A to B. The middle panel shows the radar reflectivity (in dBZ) observed by CloudSat. The lower panel is the simulated reflectivity from the model outputs.

5. Concluding comments

New observations are described that, although preliminary, offer the potential for a deep level of assessment of model moist physics. These observations provide cloud vertical structure, information about precipitation and the water and ice contents of cloud layers. It was also shown how the observations can be used to probe critical processes that, through necessity, are parameterized in models in ways that remain untested. These observations when connected to advances in modeling should provide a pathway to measurable improvements in the representation of model moist physics.

6. References

Haynes, J. and G.L. Stephens, 2007; Tropical cloudiness and the incidence of precipitation: Early results from CloudSat, to appear in *Geophys.Res.Lett.*

Haynes et al., 2007; A multi-purpose radar simulator package: Quickbeam, submitted to *Bull. Amer. Met. Soc.*

Jakob, C and G.Tselioudis, 2003; How representative are the cloud regimes at the TWP sites? - An ISCCP perspective; *Proceedings from the ARM Science Team Meeting*, Broomfield,

Mace, G. G., R. Marchand and G. L. Stephens, 2007; Global Hydrometeor Occurrence as Observed by CloudSat; Initial Observations from Summer 2006, appears in *Geophys. Res. Lett.*

Stephens, G. L., et al.,, 2002: The CloudSat mission and the A-TRAIN: A new dimension to space-based observations of clouds and precipitation. *Bull. Am. Met. Soc*., **83**, 1771-1790

Webb et al., 2002 Webb, M. J., C. Senior, S. Bony and and J-J Morcrette, 2001: Combining ERBE and ISCCP data to assess clouds in the Hadley Centre, ECMWF and LMD atmospheric climate models. *J. Clim. Dynamics*, **17**, 905-922.

Wu, D. et al., 2007; Aura MLS Cloud Ice Measurements and Comparisons with CloudSat and Other Correlative Data, submitted to *J.Geophys.Res*.